

Spin relaxation rates in quasi-one-dimensional coupled quantum dots

C. L. Romano*,¹ P. I. Tamborenea,¹ and S. E. Ulloa²

¹*Department of Physics “J. J. Giambiagi”, University of Buenos Aires, Ciudad Universitaria, Pab. I, C1428EHA Buenos Aires, Argentina*

²*Department of Physics and Astronomy, and Nanoscale and Quantum Phenomena Institute, Ohio University, Athens, Ohio 45701-2979*

(Dated: July 15, 2018)

We study theoretically the spin relaxation rate in quasi-one-dimensional coupled double semiconductor quantum dots. We consider InSb and GaAs-based systems in the presence of the Rashba spin-orbit interaction, which causes mixing of opposite-spin states, and allows phonon-mediated transitions between energy eigenstates. Contributions from all phonon modes and coupling mechanisms in zincblende semiconductors are taken into account. The spin relaxation rate is shown to display a sharp, cusp-like maximum as function of the interdot-barrier width, at a value of the width which can be controlled by an external magnetic field. This remarkable behavior is associated with the symmetric-antisymmetric level splitting in the structure.

Spin-related phenomena in semiconductors attract much attention as they are the foundation of the emerging fields of *spintronics*¹ and *quantum computing* in semiconductor systems.² Quantum dots (QD) are particularly promising since they offer relatively long spin coherence times, a key requirement in quantum information processing. Electron spin relaxation in QDs has been studied recently theoretically^{3,4,5,6,7,8,9,10,11,12,13,14,15,16,17,18,19,20,21,22,23,24} and experimentally.^{25,26,27,28,29} In this letter, we study spin relaxation rates in coupled double QDs, a type of structure that offers a very useful control parameter, i.e. the interdot separation, or barrier width. In particular, we consider here quasi-one-dimensional (quasi-1D) dot structures produced in *nanowhiskers* or *nanorods* studied experimentally. We have recently studied the electronic states of such quasi-1D double dots,³⁰ and analyzed the spin-mixed character that arises from the spin-orbit (SO) interaction. These structures can be designed so that only the Rashba SO interaction (enabled by *structural* asymmetry) is present.³⁰ In this paper, we calculate rates of spin transitions induced by phonon scattering between Rashba spin-mixed states, taking into account the different acoustic-phonon modes present in zincblende semiconductors. We find that the spin relaxation rate shows a strong dependence on the interdot-barrier width and can, furthermore, be tuned with an external magnetic field. This provides interesting flexibility in the control of electronic spin states.

Let us denote by z the coordinate in the longitudinal direction of the quasi-1D coupled double quantum-dot structure. $V_z(z)$ is the confining potential that defines the pair of coupled QDs. We assume a narrow whisker width of 2-5 nm, that each dot has a length of 30 nm, and take the width of the barrier between dots as a variable parameter. For the case of Rashba interaction,^{30,31,32}

and introducing a weak magnetic field in the z direction that breaks the spin degeneracy (but produces no diamagnetic shift), the Hamiltonian takes the form³⁰

$$H = \frac{\mathbf{P}^2}{2m^*} + H_R + \frac{1}{2}g\mu_B B\sigma_z, \quad (1)$$

where $\mathbf{P} = (P_x, P_y, P_z)$, and $\sigma = (\sigma_x, \sigma_y, \sigma_z)$ is the Pauli matrix vector.³³ After taking average $\langle \dots \rangle$ over the ground states of the lateral-confining potentials, the SO term becomes^{30,34}

$$H_{1dR} = \frac{\gamma_R}{\hbar} p_z \left\langle \frac{\partial V_x}{\partial x} \right\rangle (\sigma_x - \sigma_y), \quad (2)$$

where γ_R is material specific.

We diagonalize the Hamiltonian to take full account of the SO effects, which result in spin mixing of eigenstates. We calculate relaxation rates due to acoustic-phonon scattering between the ground state and the next two energy eigenstates in InSb and GaAs QDs via Fermi's Golden Rule:

$$\Gamma_{i \rightarrow f} = \frac{2\pi}{\hbar} \sum_{\mathbf{Q}, \alpha} |\langle f | U_{Q, \alpha} | i \rangle|^2 n \delta(\Delta E - \hbar\omega_\alpha), \quad (3)$$

where $\mathbf{Q} = (q_x, q_y, q_z) = (\mathbf{q}, q_z)$ is the phonon momentum; α indicates the acoustic phonons, and includes longitudinal, ℓ , and transverse, $t = \text{TA1}$ and TA2 modes; $\Delta E = E_f - E_i$; and n is the Bose-Einstein phonon distribution with energy $\hbar\omega_\alpha = \hbar c_\alpha Q$. $\langle f |$, $\langle i |$ are the final and initial states obtained by exact (numerical) diagonalization of the Hamiltonian. The potential $U_{q, \alpha}$ includes both deformation $\Xi_\ell(\mathbf{Q})$ and piezoelectric $\Lambda_\ell(\mathbf{Q})$ contributions:³⁵

$$U_{q, \alpha = \ell, t} = (\Xi_\ell(\mathbf{Q}) + i\Lambda_{\ell, t}(\mathbf{Q})) e^{i\mathbf{Q} \cdot \mathbf{r}}. \quad (4)$$

For zincblende semiconductors, the phonon potentials read (in cylindrical coordinates):²⁴ $\Xi_\ell(\mathbf{Q}) = \Xi_0 \sqrt{\frac{\hbar}{2DV_{c\ell}}} \sqrt{Q}$, $\Lambda_\ell(\mathbf{Q}) = \frac{6\pi e\hbar_{14}}{\kappa} \sqrt{\frac{\hbar}{2DV_{c\ell}}} \sin(2\phi) \frac{q^2 q_z}{Q^{7/2}}$, $\Lambda_{\text{TA1}}(\mathbf{Q}) = \frac{4\pi e\hbar_{14}}{\kappa} \sqrt{\frac{\hbar}{2DV_{\text{CTA}}}} \cos(2\phi) \frac{q q_z}{Q^{5/2}}$ and $\Lambda_{\text{TA2}}(\mathbf{Q}) =$

*carlu@df.uba.ar

$\frac{2\pi eh_{14}}{\kappa} \sqrt{\frac{\hbar}{2DVc_{TA}}} \sin(2\phi) \frac{q^3}{Q^{7/2}} (2\frac{q_z^2}{q^2} - 1)$, where Ξ_0 and eh_{14} are the bulk constants, κ is the dielectric constant, D is the mass density, V is the volume, and c_ℓ , $c_{TA1} = c_{TA2} = c_{TA}$ are the sound velocities for each mode.

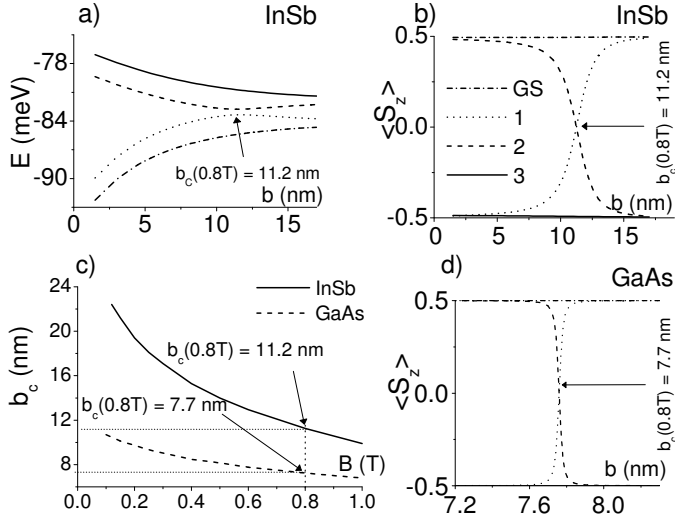


FIG. 1: Energy levels (a) and mean value of S_z (b) for the four lowest-energy eigenstates as function of the width of the central barrier, b , for InSb at $B = 0.8$ T. Notice states 1 and 2 anticross and switch spin at $b_c(B)$. (c) shows the crossing barrier b_c vs magnetic field for GaAs and InSb QDs. Panel (d) is the same as (b) but for GaAs.

For all the calculations reported here we assume a temperature of 298 K and a Rashba structural parameter, $\langle \frac{\partial V_x}{\partial x} \rangle = 5$ meV/nm.³⁶ In Fig. 1(a) (and 1(b)) the four lowest energy levels (and mean value of S_z) are shown as function of the width of the central barrier, b , for a magnetic field $B = 0.8$ T, and fixed dot size. We note that levels 1 and 2 show an anticrossing at a barrier width value where the S_z values switch, $b_c(0.8 \text{ T}) = 11.2$ nm, seen in Fig. 1(b). At low b -values, state 1 is the spatially-symmetric double-dot state with spin down, while state 2 is the spatially-antisymmetric state with spin up. Increasing barrier width decreases the symmetric-antisymmetric splitting, allowing SO to produce strong mixing, which results in the anticrossing and spin-switching we see in Fig. 1. This “crossing value” is magnetic field dependent, as shown in Fig. 1(c) for InSb and GaAs, and shows a monotonic drop with increasing B , as one would expect.

Figure 2 shows the contributions to the spin relaxation (SR) rate in InSb and GaAs coupled QDs due to the four different acoustic-phonon couplings: deformation (DP), piezoelectric longitudinal (LA), and transverse (TA1 and TA2) potentials. The rates shown correspond to the transition between the two lowest-energy states (as in Fig. 1(a)). In InSb QDs, we note that the SR rate is dominated by the deformation potential while in GaAs, it is dominated by the piezoelectric TA1 potential.²⁴ Notice that in InSb QDs, the contributions from the piezo

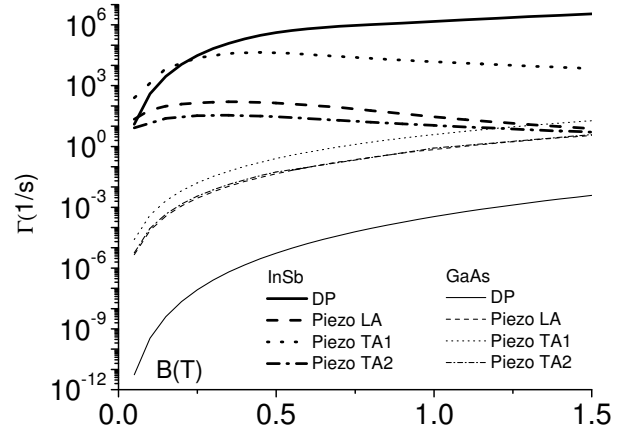


FIG. 2: Spin relaxation rates from different acoustic-phonon potentials: deformation (DP), piezoelectric longitudinal (Piezo LA), and transverse 1 (Piezo TA1) and 2 (Piezo TA2) potentials, for InSb (thick lines, upper four curves) and GaAs (thin lines) QDs as function of applied magnetic field. Barrier width $b = 30$ nm.

TA2 and LA are several orders of magnitude weaker than the others for magnetic fields beyond ~ 0.3 T. The same is true of the deformation potential in comparison to the other mechanisms in GaAs. The strong SO interaction (smaller bandgap) in InSb, results in much higher SR rates for that material than for GaAs, as one can observe in Fig. 2.

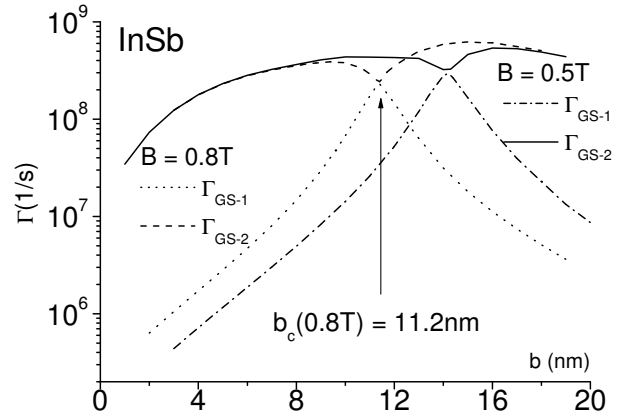


FIG. 3: Spin relaxation rate as function of central barrier width in InSb QDs, for two different values of the magnetic field ($B = 0.5$ and 0.8 T), and different transitions: from ground to first excited state (GS-1), and to second excited state (GS-2).

Figure 3 shows the *total* transition rate from the ground state to the first excited state (GS-1) and to the second excited state (GS-2) for InSb QDs and two values of the magnetic field, $B = 0.5$ and 0.8 T. We see that for a given field, the rate GS-1 shows a cusp at a barrier width that coincides with the crossing width, b_c , as introduced in Fig. 1. Accordingly, the cusp position in Γ shifts

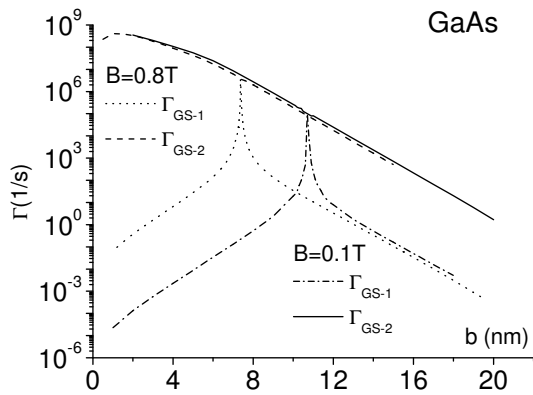


FIG. 4: Same as Fig. 3 but for GaAs at $B = 0.1$ and 0.8 T.

down with increasing magnetic field. An analogous situation can be seen in Fig. 4 for GaAs QDs, with $B = 0.1$ and 0.8 T. Here the cusp is sharper than for InSb, in correspondence with the weaker SO, as shown in Figs. 1(b) and 1(d). It must be noted that the transition GS-1 is not strictly speaking a “spin-flip” transition, since the states involved are not spin eigenstates. Indeed, the GS is

practically a pure spin-up state (Fig. 1(b)) but the state 1 has a strong spin admixture, and switches from being mostly spin-down to mostly spin-up as a function of the barrier width, b . The middle point in this transformation is given by b_c , where the cusp in the transition rate occurs. The Γ_{GS-2} values, on the other hand, show a slight dip at the same b_c position, reflecting also the mixed spin character of the 2 state. The appearance of the cusp on the lowest-energy SR rates clearly arises from the enhanced level mixing when the symmetric-antisymmetric states anticross in the double QD.

To summarize, we have studied the phonon-mediated electronic transitions between (Rashba-SO) spin-mixed states in GaAs and InSb coupled QDs. This rate shows a cusp-like maximum as a function of the separation between the dots. The position of this maximum can be controlled with a small external magnetic field, and can in principle be used to significantly change the electronic SR rates in the system.

We thank C.F. Destefani, R. Romo, C. Büsser, and M. Zarea for useful discussions, and support from CMSS at OU, UBACyT 2004-2007, ANPCyT 03-11609, and NSF-CONICET through a CIAM-NSF collaboration 0336431. P.I.T. is a researcher of CONICET.

-
- ¹ I. Zutic, J. Fabian, and S. Das Sarma, Rev. Mod. Phys. **76**, 323 (2004).
 - ² D. Loss and D. P. DiVincenzo, Phys. Rev. A **57**, 120 (1998).
 - ³ A. V. Khaetskii and Y. V. Nazarov, Phys. Rev. B **61**, 12639 (2000); *ibid.* **64**, 125316 (2001).
 - ⁴ S. I. Erlingsson, Yu. V. Nazarov, and V. I. Fal’ko, Phys. Rev. B **64**, 195306 (2001).
 - ⁵ I. A. Merkulov, Al. L. Efros, and M. Rosen, Phys. Rev. B **65**, 205309 (2002).
 - ⁶ C. Tahan, M. Friesen, and R. Joynt, Phys. Rev. B **66**, 035314 (2002).
 - ⁷ L. M. Woods, T. L. Reinecke, and Y. Lyanda-Geller, Phys. Rev. B **66**, 161318 (2002).
 - ⁸ G. Burkard and D. Loss, in *Semiconductor Spintronics and Quantum Computation*, edited by D. D. Awschalom, D. Loss, and N. Samarth (Springer, New York, 2002).
 - ⁹ R. de Sousa and S. Das Sarma, Phys. Rev. B **67**, 033301 (2003).
 - ¹⁰ Y. G. Semenov and K. W. Kim, Phys. Rev. B **67**, 073301 (2003).
 - ¹¹ L. S. Levitov and E. I. Rashba, Phys. Rev. B **67**, 115324 (2003).
 - ¹² A. Khaetskii, D. Loss, and L. Glazman, Phys. Rev. B **67**, 195329 (2003).
 - ¹³ B. A. Glavin and K. W. Kim, Phys. Rev. B **68**, 045308 (2003).
 - ¹⁴ S. Dickmann and P. Hawrylak, JETP Lett. **77**, 30 (2003).
 - ¹⁵ J. L. Cheng, M. W. Wu, and C. Lü, Phys. Rev. B **69**, 115318 (2004).
 - ¹⁶ Y. G. Semenov and K. W. Kim, Phys. Rev. Lett. **92**, 026601 (2004).
 - ¹⁷ V. N. Golovach, A. Khaetskii, and D. Loss, Phys. Rev. Lett. **93**, 016601 (2004).
 - ¹⁸ V. A. Abalmassov and F. Marquardt, Phys. Rev. B **70**, 075313 (2004).
 - ¹⁹ E. Tsitsishvili, G. S. Lozano, and A. O. Gogolin, Phys. Rev. B **70**, 115316 (2004).
 - ²⁰ W. A. Coish and D. Loss, Phys. Rev. B **70**, 195340 (2004).
 - ²¹ C.-H. Chang, A. G. Mal’shukov, and K. A. Chao, Phys. Rev. B **70**, 245309 (2004).
 - ²² D. V. Bulaev and D. Loss, Phys. Rev. B **71**, 205324 (2005).
 - ²³ F. Marquardt and V. A. Abalmassov, Phys. Rev. B **71**, 165325 (2005).
 - ²⁴ C. F. Destefani and S. E. Ulloa, cond-mat/0412520.
 - ²⁵ J. A. Gupta, D. D. Awschalom, X. Peng, and A. P. Alivisatos, Phys. Rev. B **59**, R10421 (1999).
 - ²⁶ T. Fujisawa, D. G. Austing, Y. Tokura, Y. Hirayama, and S. Tarucha, Nature **419**, 278 (2002).
 - ²⁷ T. Fujisawa, D. G. Austing, Y. Tokura, Y. Hirayama, and S. Tarucha Phys. Rev. Lett. **88**, 236802 (2002).
 - ²⁸ R. Hanson, B. Witkamp, L. M. K. Vandersypen, L. H. Willems van Beveren, J. M. Elzerman, and L. P. Kouwenhoven, Phys. Rev. Lett. **91**, 196802 (2003).
 - ²⁹ A. Tackeuchi, R. Ohtsubo, K. Yamaguchi, M. Murayama, T. Kitamura, T. Kuroda, and T. Takagahara, Appl. Phys. Lett. **84**, 3576 (2004).
 - ³⁰ C. L. Romano, S. E. Ulloa, and P. I. Tamborenea, Phys. Rev. B **71**, 035336 (2005).
 - ³¹ E. I. Rashba, Sov. Phys. Solid State **2**, 1109 (1960).
 - ³² Y. A. Bychkov and E. I. Rashba, JETP Lett. **39**, 78 (1984); J. Phys. C **17**, 6039 (1984).
 - ³³ The strong xy -confinement of the nanowhisker suppresses diamagnetic effects for the weak B -fields we consider here.
 - ³⁴ We consider confining potentials $V_x(x) = V_y(y)$ without inversion symmetry, a situation that also cancels the Dresselhaus SO terms (see Ref. 30).

³⁵ G. D. Mahan, *Many Particle Physics* (Plenum, New York, 1981).

³⁶ We will report the dependence of the relaxation rates on

these parameters in a separate publication.